

# Dynamical Cluster Quantum Monte Carlo Study of the Single Particle Spectra of Strongly Interacting Fermion Gases

Shi-Quan Su, Daniel E. Sheehy, Juana Moreno, and Mark Jarrell

Department of Physics and Astronomy, Louisiana State University, Baton Rouge, Louisiana 70803

(Dated: December 16, 2009)

We study the single-particle spectral function of resonantly-interacting fermions in the unitary regime, as described by the three-dimensional attractive Hubbard model in the dilute limit. Our approach, based on the Dynamical Cluster Approximation and the Maximum Entropy Method, shows the emergence of a gap with decreasing temperature, as reported in recent cold-atom photoemission experiments, for coupling values that span the BEC-BCS crossover. By comparing the behavior of the spectral function to that of the imaginary time dynamical pairing susceptibility, we attribute the development of the gap to the formation of local bound atom pairs.

One of the most exciting recent developments in correlated systems has been the observation of pairing and superfluidity of ultracold atomic fermions interacting via an s-wave Feshbach resonance [1–3]. The precise tunability of the Feshbach resonance mediated interaction allows the exploration of superfluidity for coupling extending from the BCS regime, with loosely-bound Cooper pairs, to the BEC regime, with local pairs at strong attraction. Thus such experiments provide a highly controllable setting to study phenomena that appears in a range of other systems, including neutron stars [4], quark matter [5], and correlated electronic systems such as the high temperature superconductors [6].

While the low-temperature properties of ultracold fermion gases are relatively well understood and essentially described by the BEC-BCS crossover wavefunction [2], the finite temperature behavior still presents several mysteries, particularly in the unitary regime, where the s-wave scattering length  $a_s$  between the two species of fermion diverges. At strong couplings preformed pairs are predicted to exist above the superfluid transition temperature [6], possibly yielding a *pseudogap* in the density of states [7]. But, how the pseudogap phenomena is reflected in experimental probes, such as radio frequency spectroscopy [8, 9], is still an open question.

To shed light on the spectral properties of resonantly-interacting fermion gases, we compute the single particle spectral function  $A(\mathbf{k}, \omega)$  as a function of frequency  $\omega$  and wavevector  $\mathbf{k}$ . The spectral function has recently been measured in experiments with trapped  $^{40}\text{K}$  atoms via a novel momentum-resolved generalization [10] of radio frequency spectroscopy [8, 9]. Various analytical methods have been developed to compute  $A(\mathbf{k}, \omega)$  in the BEC-BCS crossover based on the ladder approximation [11, 12], self-consistent many-body theories [13–15] and large- $N$  expansions [16]. These approaches are hampered by the lack of a small parameter in the unitary regime.

In this letter we combine the Dynamical Cluster Approximation [17, 18] and the Maximum Entropy Method [19] to obtain the spectral function in the thermodynamic limit without uncontrollable approximations (see also Ref. [20]). We observe a strong suppression of

low-energy spectral weight in conjunction with the expected onset of pairing correlations. Our simulations also capture the concomitant formation of a double-peak structure in  $A(\mathbf{k}, \omega)$  with decreasing temperature in the strong-coupling regime. At unitarity, we find a momentum distribution  $n_k$  consistent with the predictions of Tan [21], and an estimate of the universal parameters  $\xi$  and  $\zeta$  characterizing the unitary Fermi gas [22].

The Dynamical Cluster Approximation (DCA), unlike conventional QMC, allows the extraction of the single-particle spectral function  $A(\mathbf{k}, \omega)$  in the thermodynamic limit. One disadvantage of the DCA in the present setting is that it applies to lattice models, while cold atoms possess the itinerant-fermion dispersion  $\epsilon_{\mathbf{k}} = k^2/2m$ . However, we address this by focusing on the *dilute limit* of the three-dimensional cubic Hubbard model

$$\hat{H} = -t \sum_{\langle i,j \rangle, \sigma} \hat{c}_{i\sigma}^\dagger \hat{c}_{j\sigma} + U \sum_i \hat{n}_{i\uparrow} \hat{n}_{i\downarrow} - \mu \sum_{i\sigma} \hat{n}_{i\sigma}, \quad (1)$$

where  $\hat{c}_{i\sigma}$  annihilates a spin- $\sigma$  fermion at site  $i$ , the angle brackets restrict the sum over nearest neighbor sites with the matrix element  $t$ , and  $U$  is the attractive on-site interaction. Here, the chemical potential  $\mu$  is tuned to keep the filling at the small value  $\langle n \rangle = 0.3$ , where  $\langle n \rangle = 1$  is half filling. The Fermi energy associated with this filling is  $E_F = 3.414t$ . In this dilute limit, the hopping dispersion  $\epsilon_{\mathbf{k}} = 2t[3 - \sum_{i=x,y,z} \cos k_i]$  can be approximated by its low  $\mathbf{k}$  expansion  $\epsilon_{\mathbf{k}} \simeq tk^2$ , thus describing free fermions if we take  $t = 1/2m$ .

By tuning  $U$  close to  $U_c = -7.92t$ , the interaction strength where a two-body bound state forms in vacuum [23], we can capture the unitary regime in cold Fermi gases. We expect that interaction effects are insensitive to the underlying lattice when the scattering length

$$a_s = \frac{UU_c}{8\pi t(|U| - |U_c|)}, \quad (2)$$

exceeds the lattice spacing. We find, as discussed below, that Eq. (1) works well in the BCS and unitary regime, but begins to deviate from the free-fermion results in the deep-BEC regime of tightly-bound *local* pairs where lattice effects cannot be neglected.

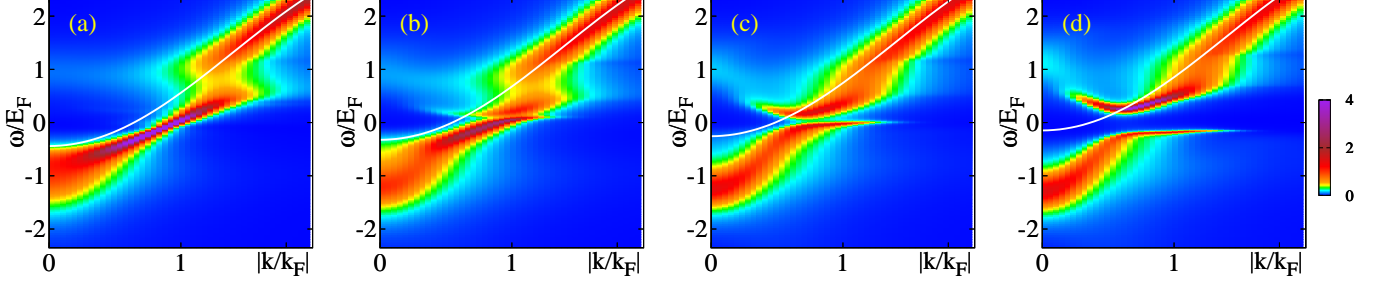


FIG. 1: (color online) The spectral function  $A(k, \omega)$  of the three-dimensional attractive Hubbard model with filling  $\langle n \rangle = 0.3$ , at temperature  $T/E_F = 0.049$ , and several coupling strengths. (a) On the BCS side of the Feshbach resonance,  $U = -6.88t$ ,  $1/(a_s k_F) = -0.99$ . (b) At unitary coupling,  $U = U_c = -7.92t$ ,  $1/(a_s k_F) \rightarrow 0$ . (c) On the BEC side of the Feshbach resonance,  $U = -8.4t$ ,  $1/(a_s k_F) = 0.38$ . (d) In the BEC region,  $U = -9.2t$ ,  $1/(a_s k_F) = 0.92$ . In each panel, the white curve is the noninteracting dispersion  $\epsilon_k - \mu$ .

The DCA covers the lattice with clusters of  $N_c = L_c^3$  sites using periodic boundary conditions. Correlations up to length  $L_c$  are considered exactly while long range correlations are treated at the mean-field level [17, 18]. We use the Hirsch-Fye quantum Monte Carlo (QMC) algorithm [24] as the quantum solver [25], and the maximum entropy method [19] to analytically continue the imaginary-time spectra to real frequencies. In the DCA the momentum resolution of the self energy  $\Sigma$  is determined by a set of  $N_c$   $K$ -points corresponding to the cluster reciprocal space [18]. We use a Fourier Transform interpolation scheme to approximate  $\Sigma$  on other  $k$ -points in the Brillouin zone. We use a Betts cluster [26] with  $N_c = 24$ . Our Hirsch-Fye QMC algorithm is efficient as long as  $|U|$  is below the bandwidth  $12t$ , allowing us to study the BEC-BCS crossover but not the asymptotic BEC limit.

We have obtained the single-particle spectral function  $A(\mathbf{k}, \omega) = -\frac{1}{\pi} \text{Im} G(\mathbf{k}, \omega)$ , with  $G(\mathbf{k}, \omega)$  the retarded Green's function, across the BEC-BCS crossover and for a wide range of temperatures. Our displayed results are along the line connecting the center of the first Brillouin zone  $\Gamma = (0, 0, 0)$  to the corner  $\mathbf{K} = (\pi, \pi, \pi)$ , with  $k$  referring to the wavevector magnitude. The spectral function along other directions is qualitatively equivalent. We focus on the large scattering length limit with  $-1 \lesssim \frac{1}{k_F a_s} \lesssim 1$ , where we approximate the Fermi wavelength  $k_F$  by the itinerant-fermion formula  $k_F = (3\pi^2 n)^{1/3}$ . Our simulations are in the normal state, meaning we cannot fully describe the broken symmetry state below the superfluid transition at  $T_c$ . Above  $T_c$ , however, expect our results to be quantitatively accurate. Previous work [23] has demonstrated that Eq. (1) yields reliable results for the transition temperature of itinerant superfluid Fermi gases. By taking the extrapolated transition temperature  $T_c$  from Ref. 23 we get  $T_c \simeq 0.064 E_F$  at unitarity coupling and filling  $\langle n \rangle = 0.3$ .

The most striking feature of our results, shown in Fig. 1, is the strong suppression of the spectral weight near zero frequency with increasing attraction towards the BEC limit. Fig. 1 displays results for four coupling values at the temperature  $T/E_F = 0.049$ . In all plots, the behavior at high- $k$  is an artifact of the underlying lattice that we shall ignore; this is reasonable since experiments only probe the occupied part of the spectral function. Fig. 1a, in the weak-coupling BCS regime ( $\frac{1}{k_F a_s} = -0.99$ ), shows an essentially free-particle dispersion for  $k < k_F$  and  $\omega < 0$ . The narrowing of the linewidth as the Fermi surface is approached from  $k \rightarrow k_F^-$  is clearly seen, consistent with the system being a Fermi liquid in this regime. With increasing coupling a two branch structure begins to form at the Fermi surface. While this behavior is barely visible at the unitary point,  $\frac{1}{k_F a_s} = 0$ , shown in Fig. 1 (b), it increases in magnitude with increasing interaction strength, as seen in panels (c) and (d). In Fig. 1(d), the deep BEC limit, the two branches of the spectral function are clearly visible, and qualitatively consistent with the recent cold-atom photoemission experiments [10].

To examine the onset of the pseudogap with decreasing temperature, we plot  $A(k, \omega)$  at fixed  $k$  as a function of energy in Fig. 2. For each coupling we have chosen the value of momentum  $k$  for which the distance between the two spectral branches is the shortest. We find the pseudogap, with decreasing  $T$ , only for coupling values beyond the unitary point. In the BEC regime, as seen in Fig. 2, the high temperature spectral functions show a Gaussian shape at high temperatures that develops a pseudogap at lower temperatures. The pseudogap separates two asymmetric peaks, reminiscent of recent analytic results [12]. We define the pseudogap  $\Delta$  as one-half the minimum peak-to-peak distance between the two spectral function peaks; our values for  $\Delta$  at the lowest temperature (characterizing the evolution of the pseudogap

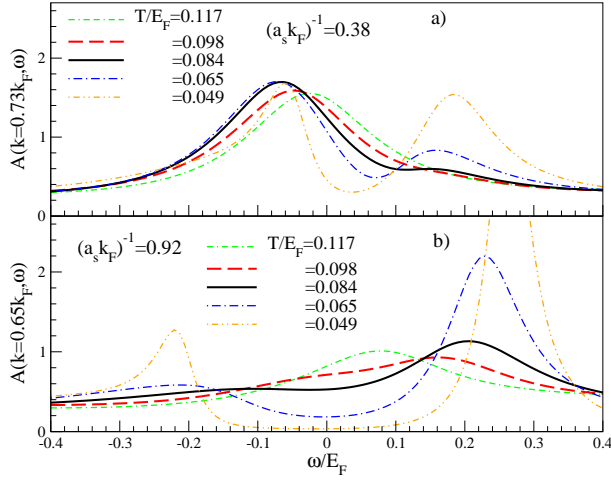


FIG. 2: (color online) Plots of  $A(k, \omega)$  at fixed momenta as a function of frequency at successive decreasing temperatures, for a) Close to unitarity ( $\frac{1}{k_F a_s} = 0.38$ ) and b) in the deep BEC regime ( $\frac{1}{k_F a_s} = 0.92$ ). Since we expect superfluidity only below  $T_c \lesssim 0.064 E_F$  [23], the suppression of spectral weight above this temperature represents the pseudogap.

across the BEC-BCS crossover) are plotted in Fig. 3(b).

Even though our simulation does not explore the superfluid state, it is able to capture the onset of pairing correlations and estimate the universal parameters  $\xi$  and  $\zeta$  characterizing the unitary Fermi gas [22]. For example, the internal energy per particle can be expressed as

$$E/N = \frac{3}{5} E_F \left[ \xi - \frac{\zeta}{k_F a_s} + \mathcal{O}\left(\frac{1}{(k_F a_s)^2}\right) \right]. \quad (3)$$

near unitarity [22, 27]. We quantify  $\xi$  from our extracted values of  $\mu$ , that is adjusted to always keep filling  $\langle n \rangle = 0.3$ . Fig. 3(a) displays  $\mu$  as a function of coupling. The chemical potential is positive and close to  $E_F$  in the BCS regime and reduces monotonically with increasing attraction towards the BEC limit of local pairing. We find  $\mu/E_F = 0.31$  at unitarity, yielding our prediction for the universal parameter  $\mu/E_F = \xi = 0.31$ , which is consistent with recent experimental and theoretical results, see e.g. Refs. [2, 28].

We also calculate the momentum distribution

$$n(k) = \int_{-\infty}^{\infty} d\omega n_F(\omega) A(k, \omega), \quad (4)$$

with  $n_F(\omega) = \frac{1}{1 + e^{\beta\omega}}$  the Fermi function. The momentum distribution has been previously measured in the BEC-BCS crossover [29]. Fig. 3(c) displays our results for  $n(k)$  showing the expected behavior: a sharp step in  $n(k)$  in the BCS regime that broadens with increasing attraction towards the BEC limit. To gain additional insight, we fit these curves to  $c_0 + c_1/(|k/k_F| + c_2)^4$  to test

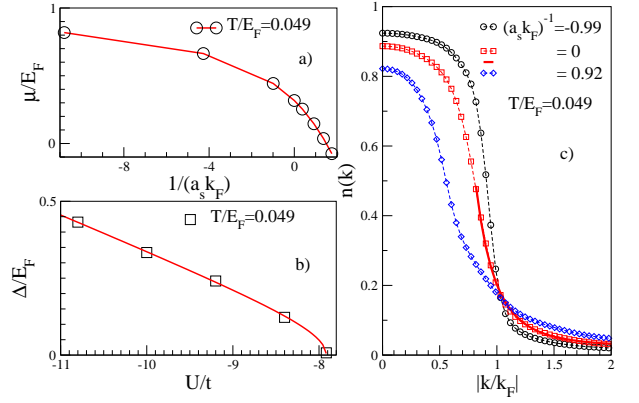


FIG. 3: (color online) (a) Chemical potential  $\mu$  as a function of coupling at  $T/E_F = 0.049$ . (b) The pseudogap  $\Delta$  extracted from  $A(\mathbf{k}, \omega)$  (square symbols). (c) Momentum distribution  $n(\mathbf{k})$  for different values of  $1/(a_s k_F)$ . The dashed lines are used to guide the eye, and the unitarity curve has been fit at large  $k$  to the Tan relation [21].

whether the Tan relation [21]

$$n(k) = C/k^4, \text{ for } k \rightarrow \infty, \quad (5)$$

governing the large  $k$  behavior of the momentum occupation, holds for our system. Although our system mimics a free-fermion dispersion at small momenta, at large  $k$  lattice effects become inescapable, and it is not clear if the Tan relation will be valid since it probes the extremely short distance behavior of interacting fermions. Despite this, we find that, at unitarity, the optimal fitting parameters are  $c_0 = 0.019$ ,  $c_1 = 0.148$  and  $c_2 = -0.057$ . The  $c_0$  and  $c_2$  are reasonably small and the fit, shown as a solid curve for the unitary plot in Fig. 3(c), is seen to be quite accurate, showing that our system does exhibit the universal properties of a unitary Fermi gas. From the theoretical relation  $c_1 = 2\zeta/5\pi$ , with  $\zeta$  governing the interaction dependence of the energy per particle near unitarity [21] (Eq. (3)), we extract the prediction  $\zeta \simeq 1.16$ . In the BCS and BEC regimes, the best-fit values of  $c_0$  and  $c_2$  are larger, so that we do not find a good fit to the Tan formula. In particular in the deep BEC region, one expects significant occupation of high momentum states. While this certainly occurs in our system, the finite size of our momentum-space Brillouin zone restricts the possible occupied momenta, preventing our system from truly accessing the deep BEC limit.

It is natural to assume that the pseudogap observed in our single-particle spectra arises from the formation of s-wave pairing correlations. To test this assumption, we study the local s-wave pair susceptibility  $\chi^s(R, \tau)$  at spatial distance  $R = i - i'$  and imaginary time  $\tau$ . Setting  $R = 0$  and  $\tau = \beta/2$ , we have

$$\chi^s(0, \beta/2) = \frac{1}{N_c} \sum_i \langle \Delta_s^\dagger(i, \beta/2) \Delta_s(i', 0) \delta_{i, i'} + h.c. \rangle, \quad (6)$$

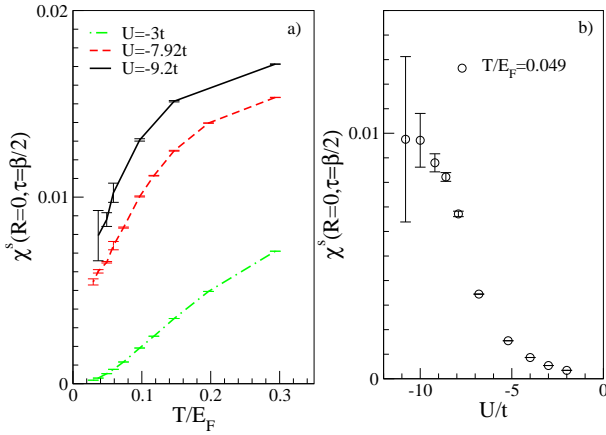


FIG. 4: (color online) Local on-site pairing susceptibility  $\chi^s(R=0, \beta/2)$  (a) as function of temperature  $T$  for different couplings and (b) as function of coupling  $U$  for  $T/E_F = 0.049$ .

where  $\Delta^s(i, \tau) = c_{i\uparrow}(\tau)c_{i\downarrow}(\tau)$  is the s-wave pair operator and the average occurs over system sites. This quantity,  $\chi^s(0, \beta/2)$ , probes local pairing correlations with the longest distance along the imaginary time direction.

In Fig. 4, we plot  $\chi^s(0, \beta/2)$  as function of temperature (left panel) and coupling (right panel). On panel (a), we can see that  $\chi^s(0, \beta/2)$  vanishes when  $T \rightarrow 0$  at weak coupling. This signals that, in the weak coupling region, atoms can not form stable local pairs; although, of course, Cooper pairing correlations will set in at very much lower temperatures, outside the range of our computational results. When  $|U|$  is large enough, towards the BEC limit,  $\chi^s(0, \beta/2)$  shows a *finite*  $U$ -dependent intercept in the zero temperature limit, showing the establishment of local pairs. Fig. 4(b) shows the coupling dependence of  $\chi^s(0, \beta/2)$  at low temperatures. While this quantity is small at weak coupling in the BCS regime, near unitarity it undergoes a rapid increase as local pairing is established.

To summarize, we have demonstrated that the Dynamical Cluster Quantum Monte Carlo, along with the Maximum Entropy Method, may be used to make quantitatively-reliable predictions for the single-particle spectral function of unitary Fermi gases. Our spectral function results capture features seen in recent  $^{40}\text{K}$  photoemission experiments [10]. We find the onset of a pairing pseudogap with decreasing temperature (above the expected superfluid transition temperature) for coupling values beyond the unitary point in the BEC regime. Since our method treats the short range correlations of the system exactly, it holds particular promise for obtaining quantitatively accurate predictions for radio frequency spectra and photoemission data in the strongly-interacting unitary regime of superfluid Fermi gases. Future work will extend this method to incorporate the effect of a background trapping potential, a necessary step

to quantitatively understand experimental results.

We acknowledge useful discussions with Dana Browne, Ehsan Khatami, Karlis Mikelsons, Unjong Yu, and Zhaoxin Xu. This research was supported by an allocation of computing time from the Ohio Supercomputer Center, by the NSF OISE-0952300 and the Louisiana Board of Regents, under grant No. LEQSF (2008-11)-RD-A-10.

- 
- [1] V. Gurarie and L. Radzihovsky, *Ann. of Phys.* **322**, 2 (2007).
  - [2] S. Giorgini, L.P. Pitaevskii, and S. Stringari, *Rev. Mod. Phys.* **80**, 1215 (2008).
  - [3] W. Ketterle and M. Zwierlein, in *Proc. Int. Sch. Phys. "Enrico Fermi"* **164**, ed. by M. Inguscio, W. Ketterle and C. Salomon, (IOS Press, 2008).
  - [4] A. Gezerlis, and J. Carlson, *Phys. Rev. C* **77**, 032801(R) (2008).
  - [5] M.G. Alford et al, *Rev. Mod. Phys.* **80**, 1455 (2008).
  - [6] Q. Chen et al, *Phys. Rep.* **412**, 1 (2005).
  - [7] M. Randeria, in *Proc. Int. Sch. Phys. "Enrico Fermi"*, **136**, ed. by G. Iadonisi, J. R. Schrieffer, and M. L. Chialafalo, (IOS Press, 1998).
  - [8] C. Chin et al, *Science* **305**, 1128 (2004).
  - [9] C.H. Schunck et al, *Nature* **454**, 739 (2008).
  - [10] J.T. Stewart, J.P. Gaebler, and D.S. Jin, *Nature* **454**, 744 (2008).
  - [11] P. Massignan, G.M. Bruun, H.T.C. Stoof, *Phys. Rev. A* **77**, 031601 (2008).
  - [12] S. Tsuchiya, R. Watanabe, and Y. Ohashi, *Phys. Rev. A* **80**, 033613 (2009).
  - [13] R. Haussmann et al, *Phys. Rev. A* **75**, 023610 (2007).
  - [14] R. Haussmann, M. Punk, and W. Zwerger, *Phys. Rev. A* **80**, 063612 (2009).
  - [15] Q. Chen and K. Levin, *Phys. Rev. Lett.* **102**, 190402 (2009).
  - [16] M. Veillette et al, *Phys. Rev. A* **78**, 033614 (2008).
  - [17] M. H. Hettler et al, *Phys. Rev. B* **58**, R7475 (1998); M. H. Hettler et al, *Phys. Rev. B* **61**, 12739 (2000).
  - [18] Th. Maier et al, *Rev. Mod. Phys.* **77**, 1027 (2005).
  - [19] M. Jarrell and J.E. Gubernatis, *Phys. Rep.* **269**, 133 (1996).
  - [20] P. Magierski et al, *Phys. Rev. Lett.* **103**, 210403 (2009).
  - [21] S. Tan, *Ann. Phys.* **323**, 2952 (2008); *Ann. Phys.* **323**, 2971 (2008).
  - [22] A. Bulgac and G.F. Bertsch, *Phys. Rev. Lett.* **94**, 070401 (2005).
  - [23] E. Burovski et al, *Phys. Rev. Lett.* **96**, 160402 (2006).
  - [24] J. E. Hirsch and R. M. Fye, *Phys. Rev. Lett.* **56**, 2521, (1986).
  - [25] M. Jarrell et al, *Phys. Rev. B* **64**, 195130 (2001).
  - [26] D. D. Betts, H. Q. Lin and J. S. Flynn, *Can. J. Phys.* **77**, 353 (1999).
  - [27] J. Carlson et al, *Phys. Rev. Lett.* **91**, 050401 (2003).
  - [28] M.Y. Veillette, D.E. Sheehy, and L. Radzihovsky, *Phys. Rev. A* **75**, 043614 (2007).
  - [29] C.A. Regal, et al *Phys. Rev. Lett.* **95**, 250404 (2005).